Fibers and Polymers 2021, Vol.22, No.11, 3192-3202
DOI 10.1007/s12221-021-1386-y

ISSN 1229-9197 (print version)
ISSN 1875-0052 (electronic version)

The Influence of Substrate Functionalization for Enhancing the Interfacial Bonding between Graphene Oxide and Nonwoven Polyester

Junaid Khan and M. Mariatti*

School of Materials and Mineral Resources Engineering, Universiti Sains Malaysia, Nibong Tebal Penang 14300, Malaysia
(Received December 5, 2020; Revised January 31, 2021; Accepted February 23, 2021)

Abstract: Electronic textiles or e-textiles have become a hot topic considering the future era of wearable electronics that are expected to replace currently available non-flexible devices. Among various methods, coating carbon-based conductive fillers on the flexible fibrous surface seems to be a promising method for e-textile and many other applications. Graphene is the top candidate among other carbon forms owing to its exceptional properties and nontoxicity. The functional groups present on the fibers surface has a significant impact on the adhesion and bonding of graphene sheets, which in turn have a profound effect on forming conductive networks that lead to improved performance of the end product. In this article, graphene oxide (GO) is coated on unmodified and chemically surface modified with positively (amine) and negatively surface (alkali) charged polyester non-woven fabrics. The facile dip-coating technique was used to coat the fabrics, surface bonding, morphology, wettability, and thermal properties of the modified surfaces were thoroughly investigated. The study revealed that modification of the fibre surface leads to increased coating uptake, improved thermal properties and uniform coating coverage. The polyester modified with sodium hydroxide exhibited the best result with an improvement of 30 % for uptake and 15 % for thermal conductivity as compared with the untreated polyester demonstrating the importance of functional groups on the surface of the fibers.

Keywords: Graphene oxide, Dip coating, Functionalized polyester, Surface characteristics, Adhesion

Introduction

The invention of textiles is as old as the human civilization; however, its role is no longer limited to merely as a clothing material. It has, in fact used in various sectors in which technical properties are predominant compared to aesthetic properties that are widely classified as technical textiles. These sectors include automobiles, medical textiles, agriculture, construction materials, protective clothing and electronic textiles (e-textiles) [1-3]. Among various fields of technical textiles, e-textiles are gaining immense popularity considering future trends of wearable electronics that can function similarly to rigid and non-flexible electronic devices that are currently available. Most recent applications of technical textiles includes electricity generation, sustainable thermal interface materials and multifunctional textile materials in which conductive properties are imparted on the textile structure [4,5]. Many previous studies reported formation of conductive networks using metal wires on the textile structure, but this is not recommended since it lacks in comfort properties such as flexibility and light weight along with its concerns related to skin irritation that is due to the rigid nature of metals [6-8]. There are different ways in which conductivity can be achieved on the textile substrate; each has its own advantages and limitations. For instance, by blending an insulating polymer with conductive materials and by wet-spinning or electrospinning techniques, but these method involves the use of costly materials; hence, it cannot be used for commercialization [9-12]. Another approach involves direct fabrication of conducting fibers, but its synthesis involves use of harsh chemicals such as strong acids and coagulants [13]. Coating textile fibers with highly conductive, lightweight, and non-toxic materials, such as graphene, seems to be a feasible and facile approach for the purpose of maintaining the comfort and mechanical properties without losing conductive properties essential for a plethora of applications.

Graphene is a sp^2-hybridized, 2D material well known for its extraordinary thermal, electrical, mechanical and optical properties that make it an ideal candidate to be used for fabricating textile-based functional materials considering properties such as high thermal and electrical conductivity, light weight, high surface area and non-toxicity [14,15]. Carbon nanotubes (CNT) also seems to be a suitable material; however, concerns related to its cytotoxicity limit its application, especially in wearable electronics [8]. Graphene oxide (GO) is a suitable candidate for coating on the textile substrate as it is cheaper than graphene and can be produced using modified Hummer's method in large quantities. Furthermore, the presence of carboxy, epoxy, and hydroxyl functional groups in the GO structure helps in bonding and results in uniform aqueous dispersion, hence eliminating solvent cost and efforts required for dispersion of nano-particles [16]. There are different methods that can be used for coating GO on the fibre surface, which include dip coating, spray coating, screen printing, vacuum filtration, inkjet printing and exhaust dyeing [17,18]. The GO after coating on the textile materials can be reduced to form graphene (rGO) to retain the conjugated structure using various natural or synthetic reducing agents. However this

*Corresponding author: mariatti@usm.my

Table 1. Summary of previous work involving substrate modification and GO/rGO coating

Substrate	Substrate modification	Effect	Reference
Polylactic acid, polyester, polypropylene and nylon	Ultraviolet ozone (UVO) treatment	Improved conductivity	[7]
Polyester	Sonication using heptane water mixture	Higher loading of GO	[8]
Polyester	Alkali treatment	Increased GO absorbancy	[20]
Bio-based polyester	Hydroxy grafted Bio-PET	Improved electrical and thermal conductivity	[32]
Cotton	Polyethyleneimine treatment	Electrostatic attraction	[36]
Polyester	Plasma and BSA protein	Improved adhesion	[37]
Nylon/lycra	Plasma and pyrrole treatment	Improved capacitance	[40]
Polyester	N-cetyl pyridinium chloride surfactant treatment	Improved adhesion	[41]
Cotton	Alkali treatment	Improved nanosheet adsorption	[42]
Polyester	Polyurethane (PU) treatment	Improved adhesion and uniformity	[43]

step is optional and is required in applications where electrical conductivity is essential [19-21]. Reports on application of GO with textile materials include application in fabrication of electro-conductive textiles, thermal interface materials, hybrid scaffolds, composite materials, multifunctional fabrics, UV blocking materials, hydrophobic fabrics, dye sensitized solar cells (DSSC), flame retardant fabrics, antibacterial fabrics, fabric sensors, supercapacitors and energy storage materials [1,22-24].

The functional groups present on the surface of the fibers play a pivotal role in the adhesion process of the coating material on the textile surface, which in turn enhances the performance of the end product as reported by many studies summarized in Table 1. These studies include synthesis of a biobased hydroxyl-terminated polyester, sonication of the substrate using a heptane and water mixture and substrate treatment with alkali, plasma, polyurethane, polyethyleneimine, ultraviolet light, and surfactant. With the current rise in the demand for e-textiles with GO as the most preferable conductive coating material, a study investigating the effect of fiber's functional groups on GO uptake, uniformity and properties would be helpful for future development in the field of e-textiles. However, after thorough literature review we found that, there is little knowledge available on this topic. In this work, an investigation was carried out by first forming surface positively and negatively charged functional groups on the PET non-woven fabric via chemical treatment through alkali (−) and amine (+) heterogeneous reaction followed by coating GO using a facile dip coating technique. The comparison between the functionalized fabrics was made with a goal to figure out the best fiber modification for uniformity and GO uptake. The effect of substrate functionalization on morphology, surface characteristics, chemical bonding, and thermal properties was investigated using various characterization techniques. This study will assist researchers working in the field of technical textiles to fabricate materials with desired properties using graphene.

Experimental

Materials

Polyester non-woven fabrics (100 GSM, 3 mm thick) were purchased from local department stores. All chemicals including sodium hydroxide (NaOH), 98 % sulfuric acid (H_2SO_4), hydrocholoric acid (HCl), potassium permanganate ($KMnO_4$), sodium nitrate ($NaNO_3$), 60 % hydrogen peroxide (H_2O_2) and graphite flakes were purchased from Merck assay. Poly(dimethylamine co-epichlorohydrin) (50 weight %) was provided by Sigma Aldrich Sdn. Bhd. Water used in this experiment was purified using a Milli-Q system with

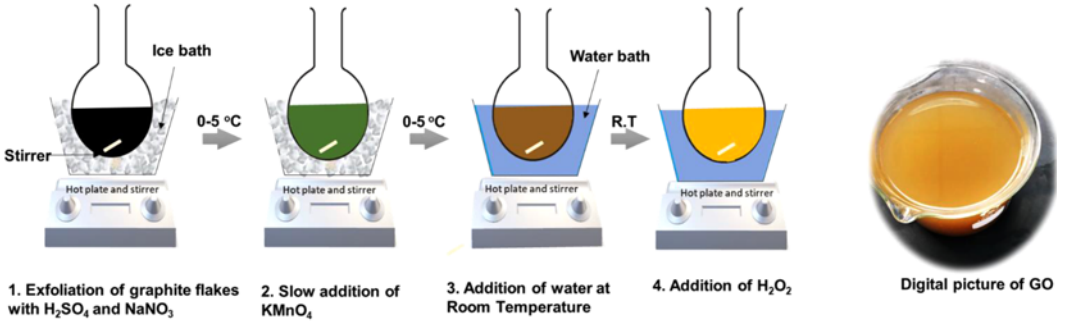

Figure 1. Schematic of the synthesis process of graphene oxide by modified Hummer's method.

resistivity higher than 18.2 M ohm cm^{-1}.

Synthesis of GO

Modified Hummer's method [25] was used to synthesize GO as represented schematically in Figure 1. Briefly, 1 g of graphite flakes and 0.5 g of $NaNO_3$ was exfoliated in 25 m*l* of 98 % concentrated H_2SO_4 for 2 h with temperature maintained at 5-10 °C using an ice bath. After that, 5 g of $KMnO_4$ was added slowly with continuous stirring for another 2 h. The temperature was brought back to room temperature, and then 70 m*l* of deionized water was added dropwise. The resultant aqueous solution was allowed to stir for another 30 min with further dilution, and then 6 m*l* of 60 % concentrated H_2O_2 was added to terminate the reaction. The resultant solution was centrifuged at 3,000 rpm several times with dilute 5 % HCl solution and deionized water for purification. The graphite oxide supernatant was dried in an oven at 60 °C and ground to form powder.

Preparation of Functionalized Fabrics

The fabric were cut into 5 cm^2 area and were sonicated in a bath-type sonicator for 20 min to make it clean and free from residual dirt and impurities. The process of fabric functionalization is represented schematically in Figure 2.

Alkali Functionalization

Alkali functionalization was carried out by aqueous solution of sodium hydroxide. Sodium hydroxide pellets was weighed accurately and dissolved in water to form 0.5 weight % aqueous solution at room temperature. The cleaned fabric was dipped in the prepared solution. The temperature of 80 °C was maintained using a hot plate with continuous stirring for 1 h. The fabrics were taken out of the solution and washed with a copious amount of water to remove the unreacted alkali followed by drying at 60 °C in a preheated oven. The fabric was labeled as FAPET for the alkali-functionalized polyester.

Amine Functionalization

The cleaned fabric was dipped in 1 % aqueous solution of poly(dimethylamine co-epichlorohydrin) for 10 min at room temperature followed by drying at 60 °C. After drying, the fabrics were washed several times with water and then dried again in the oven at 60 °C. Before the treatment of polyester with an aqueous solution of poly(dimethylamine co-epichlorohydrin), an additional step of alkali treatment meant to graft hydroxy and carboxy functional groups was carried out. The fabric was labeled as FNPET for the amine-functionalized polyester.

Preparation of GO-coated Fabrics

Graphite oxide powder was re-dispersed in deionized water to form a 0.5 weight % brown solution, and their layers were separated using the bath-type sonicator for 20 min to form a homogeneous GO solution. Functionalized non-woven fabrics are dipped in the GO aqueous solution and kept for 15 min for adsorption and then dried at 60 °C for 6 h. This process is repeated four times for maximum GO uptake. Similar procedure was also followed for unfunctionalized fabrics. The fabrics were labeled as UFPETGO, FAPETGO, and FNPETGO for unfunctionalized, alkali-functionalized, and amine-functionalized GO-coated polyester fabrics, respectively. The process followed for coating is also illustrated in the schematic of Figure 3.

Characterization Methods

Attenuated Total Reflectance Fourier-transform Infrared Spectroscopy

Synthesized GO, surface functionalization of non-woven fabrics and bonding of GO on the fabrics were confirmed by using attenuated total reflectance Fourier-transform infrared spectroscopy (ATR-FTIR) Nicolet IS10 (USA) spectrometer. The KBr pellet method was used to prepare the GO powder sample before analysis. GO powder was mixed with potassium bromide in the ratio 1:9 and pressed for 2 min at 20 psi. This procedure was not required for other samples because they were in the form of fabrics. The measurements were done at room temperature and ambient atmosphere in the range of 500-4,000 cm^{-1}.

X-ray Diffraction Analysis

X-ray diffraction (XRD) patterns were obtained using a Bruker D8 X-ray diffractometer with a Ni-filtered Cu-Kα (λ=1.54021 Å) radiation source at the range of 10 ° to 80 ° in order to confirm the oxidation of graphite flakes. The interlayer spacing of the synthesized GO was calculated

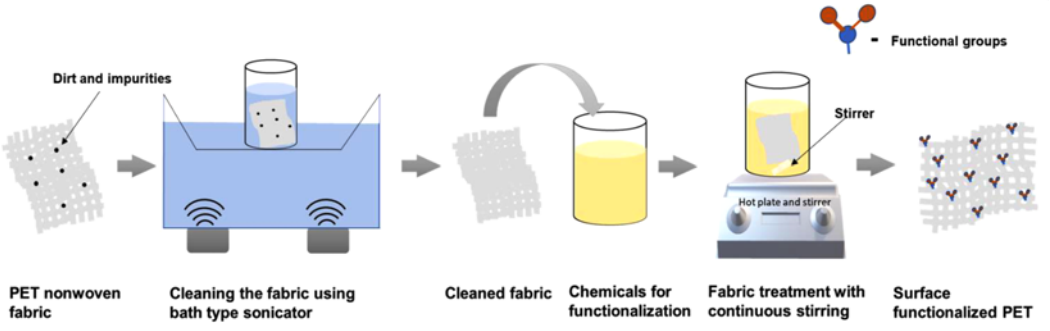

Figure 2. Schematic of the process for the functionalization of fabrics.

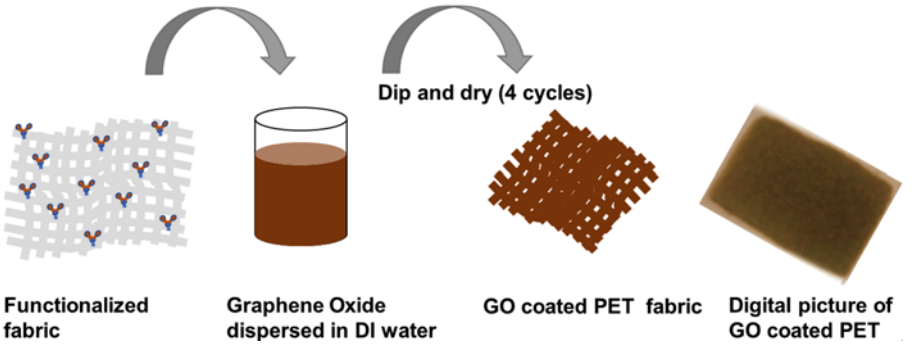

Figure 3. Schematic of the dip coating process of graphene oxide on PET fabrics.

from the peak position of the XRD spectrum using Bragg's equation given in equation (1):

$$\lambda = 2d\sin\theta \quad (1)$$

λ(Å) is the wavelength of the X-rays, d (nm) is the interlayer distance, and θ (º) is the angle between the incident ray and the scattering planes.

Scanning Electron Microscopy (SEM)

The morphologies of the GO nanoparticles that adhered on the surface of the non-woven fabrics were characterized using high-resolution field-emission scanning electron microscope (FESEM Zeiss SUPRATM 55VP). The samples were cut into small pieces and scanned at an accelerating voltage of 5 kV of different portions with various magnifications for consistency in the results.

Atomic Force Microscopy

Surface topography and parameters were examined using atomic force microscopy (AFM, Nano Navi SII) equipped with an SI-DF20 cantilever with aluminum back coating. The AFM was operated in the non-contact mode under an ambient atmosphere at room temperature. The scan range of the scanner used in this study was 10 μm×10 μm (x×y), and the height (z) is ≤1.5 μm.

Dynamic Contact Angle Test

Dynamic contact angle and tensiometer (DCAT) was used to identify contact angle and GO uptake with respect to time. The samples were prepared by filling the non-woven fabric in a tiny tube that forms capillaries, and based on the rising principle, a curve of rising mass of liquid with time was measured. The contact angle was calculated by the tensiometer software using equation (2):

$$\cos\theta = \frac{m^2 \cdot \eta}{t.\rho^2.\sigma_L.C} \quad (2)$$

where θ is the equilibrium contact angle, (º); m is the liquid mass, g; h is the viscosity of the liquid, mPas; ρ is the density, g/cm^3; L is the liquid surface tension, mN/m; t is the time, s; and C is the capillary number of the powder, obtained from hexane.

Percentage Uptake

The amount of coating taken up by a particular type of substrate was calculated by weighing the fabric before coating and after coating and complete drying overnight in an oven at 60 °C. The percentage (%) uptake was calculated using the formula given in equation (3).

$$\%\ uptake = \frac{\text{final weight} - \text{initial weight}}{\text{initial weight}} \times 100 \quad (3)$$

Thermal Conductivity

Hot disc thermal constant analyzer model TPS 2500 was used to identify thermal conductivity (k) value which is used to evaluate the formation of conductive networks. A sensor which acts as a heat source as well as detector was placed between the two samples.

Results and Discussion

Characterization of Synthesized Graphene Oxide

The oxidation of graphite to GO was confirmed using the X-ray diffraction pattern (XRD) given in Figure 4. The strong and sharp peak at 2θ=10.214 ° corresponds to the interlayer spacing of 0.86 nm, which is much greater than that of

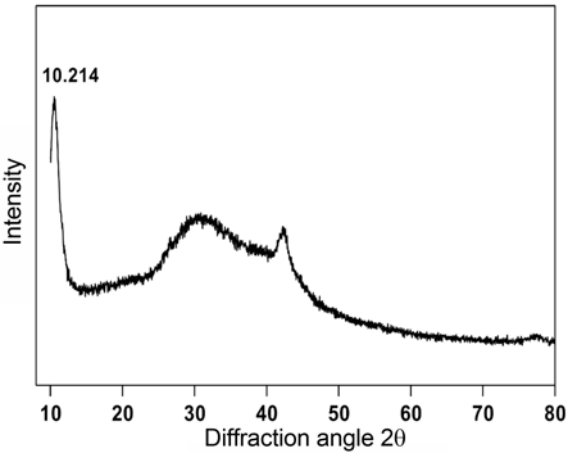

Figure 4. X-ray diffraction pattern of GO.

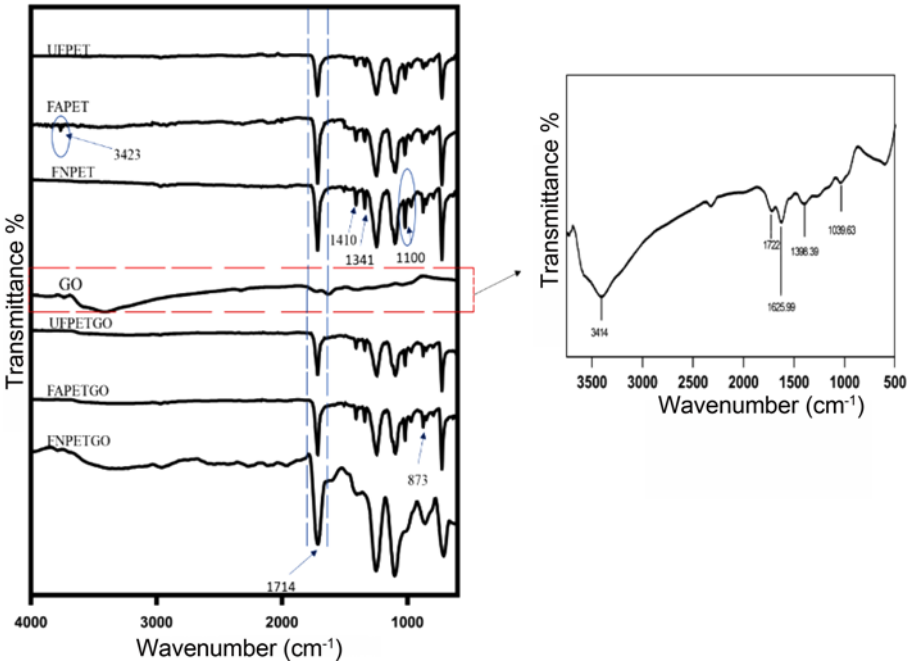

Figure 5. FTIR spectrum of non-woven fabrics and GO.

graphite (0.34 nm). This change is due to the presence of carboxyl, carbonyl, hydroxy, and epoxy functional groups on the basal plane and edges, which are responsible for an increase in the interlayer spacing of graphite sheets [19]. The XRD pattern of GO is considered to be a characteristic diffraction pattern of GO, as reported in previous studies [26]. The synthesized GO was also investigated for the presence of various functional groups using the FTIR spectrum given in Figure 5. The broad peak at 3,414 cm^{-1} can be attributed to the stretching vibrations of the hydroxyl groups (O-H). The peak at 1,722 cm^{-1} is the result of carboxy and carbonyl functional groups (C=O). The peak at 1,625 cm^{-1} can be attributed to the stretching mode of aromatic unoxidized graphite (C=C) [27]. The peak at 1,398 cm^{-1} is the result of the deformation vibration of tertiary C-OH groups. The peak at 1,039 cm^{-1} belongs to the stretching vibration of C-O functional groups [28]. The oxidation of graphite to GO is evident because of the presence of various oxygen functional groups on the GO sheets, which was also confirmed by the XRD diffraction patterns that were further used after purification in this study.

FTIR Study of PET Fabrics

To investigate the presence of functional groups on the surface of non-woven PET and bonding of GO with the substrate and its effect with carboxy and amine functionalization, FTIR analyses of UFPET, FAPET, FNPET, GO, UFPETGO, FAPETGO and FNPETGO were carried out in the range of 500 to 4,000 cm^{-1} as given in Figure 5. The characteristic sharp and strong peak at 1,714 cm^{-1} corresponds to C=O vibration. The peak at 1,410 cm^{-1} and 1,341 cm^{-1} is attributed to aromatic stretching and carboxylic, ester functional groups, respectively. The peak at 873 cm^{-1} corresponds to the hydrogen atoms of the benzene ring. There is also a weak O-H stretch at 3,753 cm^{-1}, which slightly increases after alkali functionalization [29]. The alkali-treated functionalized (FAPET) sample also shows a significant increment in the C=O stretching peak at 1,714 cm^{-1} after functionalization in the spectrum, which manifests the generation of the surface carboxyl group. The weak O-H stretching at 3,753 cm^{-1} disappears after amine treatment, which could be due to the bond formation of hydroxy groups with amine-based polymer; also, there is a slight increment in the peak at approximately 1,100 cm^{-1} that is attributed to C-N stretching, confirming the presence of positively charged nitrogen functional groups in the fabrics [30]. FTIR results clearly indicate successful functionalization of fabrics with both alkali and amine functional groups, which will be used for further investigation.

The FTIR spectrum after GO coating on the functionalized and unfunctionalized fabrics was also taken for the purpose of investigating the bonding of GO with the fabrics and plotted on the same graph for convenience of comparison, as given in Figure 5. The peak disappearance at 1,722 cm^{-1} (C=O) and 3,423 cm^{-1} (O-H) can be the result of ester bond formation between GO and PET. The same inference can be made based on the peak disappearance at 3,414 cm^{-1} (O-H) with a decrease in the peak at 1,714 cm^{-1} (C=O) for FAPETGO and UFPETGO. The ester bond formation can be understood on the basis of bond polarity differences between

the hydroxy and carboxy functional groups. These results are in agreement with previous results that indicate that surface carboxylic groups play a key role for bonding with coating materials that have a profound effect in forming conductive networks [31-33]. The results were not as straightforward for FNPETGO as those of FAPETGO and UFPETGO. The broad OH stretch of GO is retained in the FTIR spectrum of FNPETGO, which signifies that there was no bonding with the hydroxy functional groups of the GO. Further, the C=O peak has appeared to be broadened with no decrement in the peak intensity, referring to no chemical interaction with the carbonyl functional groups of PET and GO.

Morphology and Surface Characterization of GO Coating

GO coating on the fabrics can be visually detected with substrate color change from white to brown, as illustrated in Figure 6(A and B). The depth of the brown color was observed to increase with dip cycles; which was an indication of increased uptake of GO on the fabric [34]. The dip coating was meticulously performed by keeping the same conditions for all the samples so that the control condition does not cause discrepancies in the results. The distributions of GO sheets on the surface of the untreated and alkali and amine-treated fabrics look similar through our naked eyes; however, observation using FESEM showed significant differences, as illustrated in Figure 6. The fibers with GO particles adhered are clearly visible in all the samples. Notable differences were observed between the unfunctionalized and functionalized samples in terms of uniformity and particle distribution. The particles were unevenly distributed, and their agglomeration was visible, as indicated by the arrow in UFPETGO (see Figure 6(ai)). The functionalized samples (FAPETGO and FNPETGO) showed comparatively homogeneous coverage of the GO on the fabric (Figure 6(bi and ci)). The variations in the distribution of the particles on the fibre surface indicate role of surface functional groups to prevent agglomeration. Agglomeration of the particles is highly undesirable since it has detrimental effects on the properties of the materials [35]. Understanding the nature of the coating material (GO) and its interaction with the substrate (functionalized and unfunctionalized

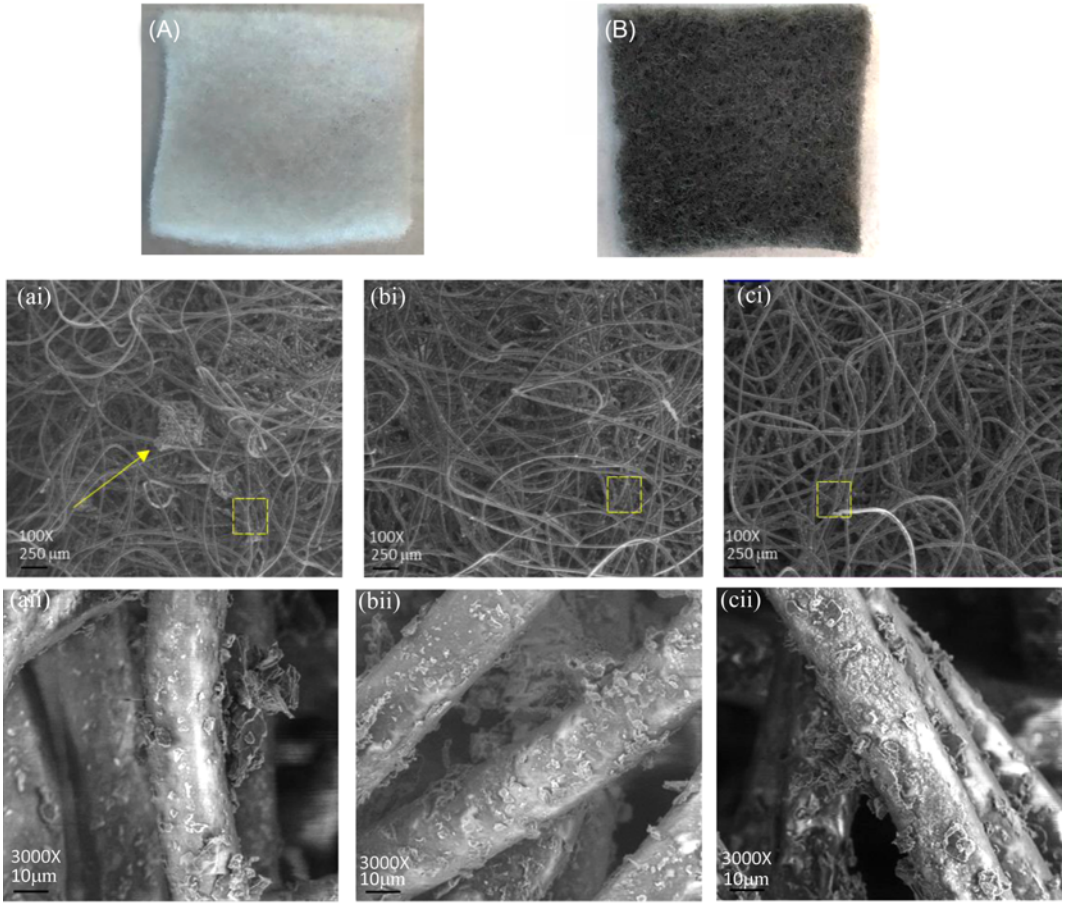

Figure 6. Digital picture of PET, (A) before coating, (B) after coating. Morphology of fabrics indicating the presence of GO particles on the surface of PET fibres of (a) UFPETGO (arrow indicating agglomeration), (b) FAPETGO, (c) FNPETGO ((i) and (ii) indicating 100X and 3000X magnifications respectively).

polyesters) can give a clearer picture of the differences.

It is a general belief that there is a strong electrostatic driving force between two particles of opposite charges that causes the attraction and leads to successful deposition of particles on the substrate, as reported by many previous reports [36,37]. However, it should be noted that there are other physical and chemical forces involved that are important in determining the particle distribution and uptake on the substrate. The interaction between the GO particles and the substrate depends on various factors, which are a topic of keen interest and are dependent on the surface chemistry of both the substrate and the coating particles. One of them is wettability, which will have a considerable influence on the % uptake. Wettability depends on the surface energy of both the substrate and the coating material. Surface energy is the excess energy at the surface, is highly dependent on the functional groups and is expected to increase with strong covalent bonds on the surface [38]. Hence, to attain more wettability, the substrate should have a contact angle < 90 º that causes the coating liquid to spread out on the substrate and is expected to increase with an increase in the hydrophilic functional groups.

The coating material (GO) is considered to be amphiphilic in nature because of the presence of hydrophilic epoxide and hydroxyl groups at the basal plane and carboxylic groups at the edges and hydrophobic polyaromatic benzene rings. The presence of both hydrophilic and hydrophobic groups gives GO the ability to have electrostatic and hydrophobic π-π interactions. GO has shown to have adhesion on all the samples irrespective of the substrate surface charge, which could be due to the hydrophilicity of GO and large surface area with micropores on the non-woven PET substrate that allows the GO solution to enter the substrate with high surface capacity that was visible by the change in color. The % uptake of each GO-coated PET sample value is given in Table 2. The alkali-functionalized sample showed the highest uptake of 31.29 %, which was not expected because there is repulsion between the GO and FAPET due to the presence of negatively charged oxygen functional groups in both the substrate and the coating material. The highest uptake is also evident from Figure 6(bii), which clearly depicts that more particles were adsorbed on the surface of FAPETGO compared to that of UFPETGO (Figure 6(aii)). The substrate wettability plays a major role in the adsorption process because more hydrophilic material will adsorb more GO particle along with formation of strong covalent bonding, which could be the reason for more uptake and excellent bonding of FAPET, considering the presence of active surface functional groups that enhances wettability. To evaluate this, a dynamic contact angle test was performed in which DI water was used as a test liquid. Marginal differences in the equilibrium contact angle were observed between the samples as given in Table 2, with the alkali-functionalized sample showing the minimum contact angle, indicating the highest hydrophilicity, whereas the highest contact angle was observed in case of FNPET, probably due to the presence of a thin polymeric layer of poly (dimethylamine co-epichlorohydrin) on the surface used for functionalization that inhibits the contact with the liquid surface. Although there are slight differences in the equilibrium contact angle, since the fabric used is non-woven and thus highly porous, the wettability of the substrate is significantly altered; this could be the reason behind the differences in the % uptake.

Table 2. Equilibrium contact angle, % uptake and thermal conductivity values of different samples

Sample name	Equilibrium contact angle (°)	% uptake	Thermal conductivity ($W\ m^{-1}K^{-1}\times10^{-3}$)
UFPETGO	88.18	14.44	43.43
FAPETGO	86.95	31.29	49.79
FNPETGO	89.77	21.97	45.03

Further, to study the interaction of GO with the substrate, GO was used as a test liquid and a graph of mass vs. time was plotted until equilibrium was reached as given in Figure 7. The graph indicates that FNPET takes the shortest time to reach the equilibrium because of the electrostatic driving force between positively charged nitrogen atoms on the substrate surface and negatively charged GO due to the presence of various oxygen moieties. The opposite charge leads to a strong electrostatic driving force that causes adhesion of GO particles; hence, equilibrium is quickly reached. However, the adhesion is strictly physical adsorption because there was no evidence in the FTIR spectrum that indicates strong covalent bonding between FNPET and GO.

The alkali-treated sample took the highest time of 22 mins to reach the equilibrium because of the electrostatic repulsion since the coating material is GO and the substrate surface is functionalized with negatively charged functional groups; however, after the equilibrium is reached, the GO

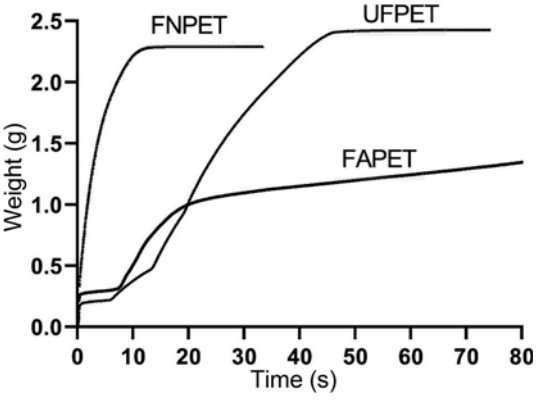

Figure 7. Graph of weight uptake vs time measured by DCAT for different samples.

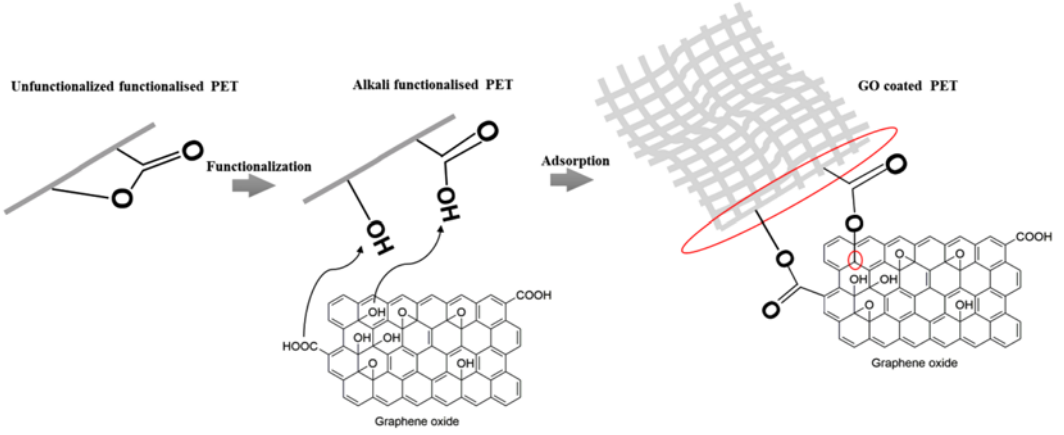

Figure 8. Schematic of the chemical adsorption process between GO and alkali modified PET.

particles formed strong bonding with the substrate as indicated in the FTIR spectrum.

The dynamic contact angle test elucidates the uptake of FNPET due to opposite charges. However, the reason for FAPET uptake can be attributed to hydrophilicity followed by formation of strong covalent bonding due to the difference in the polarity of the enhanced functional groups present on the surfaces. Figure 8 is an illustration of the chemical bonding between GO and FAPET, which was also confirmed with FTIR spectrum given in Figure 5. whereas there was no evidence of bonding of GO with FNPET. The bonding between GO and FAPET is due to the presence of carboxyl and hydroxyl functional groups that leads to esterification reaction between substrate and graphene oxide. This leads to formation of strong covalent bonding as represented schematically in Figure 8, there was no evidence of bonding in case of FNPETGO. In case of UFPET, very few particles have been shown to have good bonding with the substrate, as reflected in the FTIR spectrum which could be due to hydrogen bonding which is present in all samples. GO particles, if not anchored on the surface, will be in the form of stable dispersion due to the hydrophilic nature of GO that allows particles to be between the water molecules. However, after solvent evaporation, forces such as π-π interaction and van der Waals forces cause the particles to come closer with each other, forming clumps as observed in the SEM image in UFPETGO (Figure 6(ai)). The improvement in the thermal conductivity values with bonding and % uptake is evident from Table 2, in which FAPET exhibits the highest thermal conductivity which could be due to formation of better conductive network and more GO particles. These results demonstrate the importance of surface functional groups and charges on the adhesion behavior of the particles on the substrates.

The GO coverage on the surface of the fabric substrate was also investigated with AFM to evaluate the surface characteristics because the AFM images are capable of sensing regions that are covered with graphene and those that are exposed and to calculate surface parameters as shown in the topography images and height profiles for scanning areas of 10×10 μm, given in Figure 9. The AFM topographical 2D images showed significant differences in terms of surface coverage with GO sheets for chemically treated and untreated fabrics. The RMS roughness values of UFPET, FAPET, and FNPET are 31.57, 41.61 and 39.76, respectively, which manifest better coating of the functionalized substrate. Kurtosis values (S_{ku}) that measure the relative extent of the degree of peak distribution with respect to the normal and are a major indicator of coating surface homogeneity, and skew values that indicate the degree of asymmetry around the mean value of UFPETGO, FAPETGO, and FNPETGO are given in Table 3. The lowest kurtosis value with a negative skew value (S_{sk}) of FAPETGO indicates that the coating topography is blunt, showing more homogeneous coating of GO on the alkali-treated PET substrate [39]; however, both UFPET and FNPET have positive skew values and a comparatively higher kurtosis value suggesting sharp pointed topographies, which are also evident from their corresponding height profiles.

There are two important components in an AFM image: a low-frequency component that defines the shape of the image and a high-frequency component that defines finer details such as roughness. To further evaluate the coating on the surface of the fibers, the texture obtained in the AFM image was filtered by eliminating the low-frequency component, after which the 3D image was obtained for the high-frequency component, which gives more elaborate details of the coating as given in Figure 10. The image was processed using the freeware software Gwyddion. The coating particles were clearly visible on the surface of an individual fiber selected for the study. The results obtained by the statistical analyses of RMS surface roughness (S_q), kurtosis value (S_{ku}) and skew value (S_{sk}) and the height profiles are incongruent with the visual appearance of the

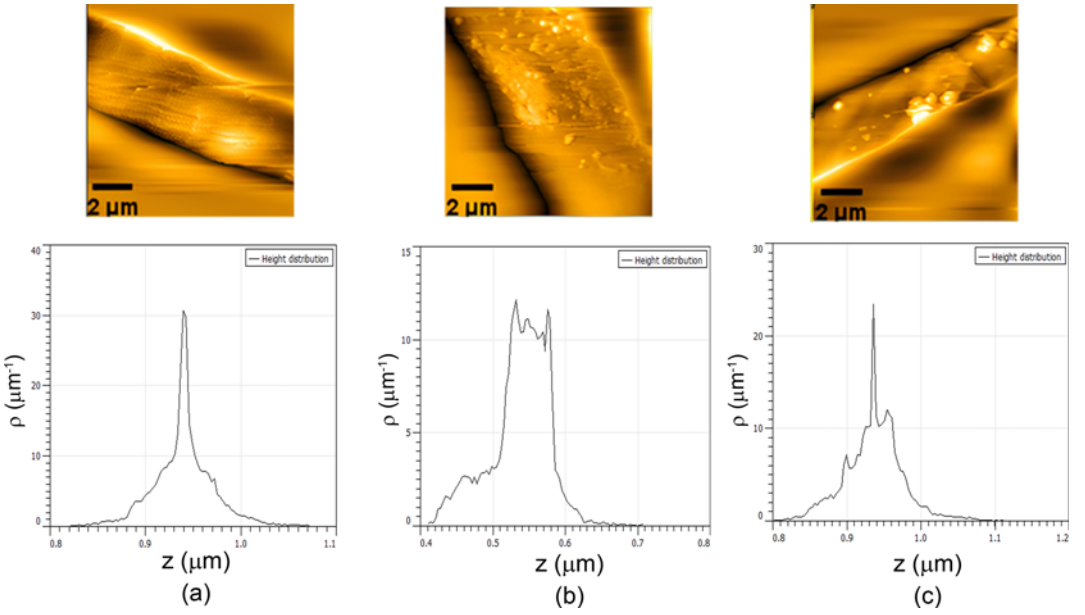

Figure 9. AFM topography 10×10 µm images of (a) UFPETGO (b) FAPETGO (c) FNPETGO and their corresponding height profiles.

Table 3. Surface parameters of samples

Sample name	RMS roughness (S_q) (nm)	Skew (S_{sk})	Kurtosis (S_{ku})
UFPETGO	31.57	0.1477	1.583
FAPETGO	41.61	-0.5068	0.5336
FNPETGO	39.76	0.1854	1.258

3D images. The coating particles were found to be of very less height with unevenness for UFPET, which matches the roughness parameters. Amine-treated sample showed better coating than UFPET but lacked in terms of homogeneity and particle coverage on the fiber surface. The best results were obtained with the alkali-coated sample, showing both more coating and homogeneous particle coverage on the surface

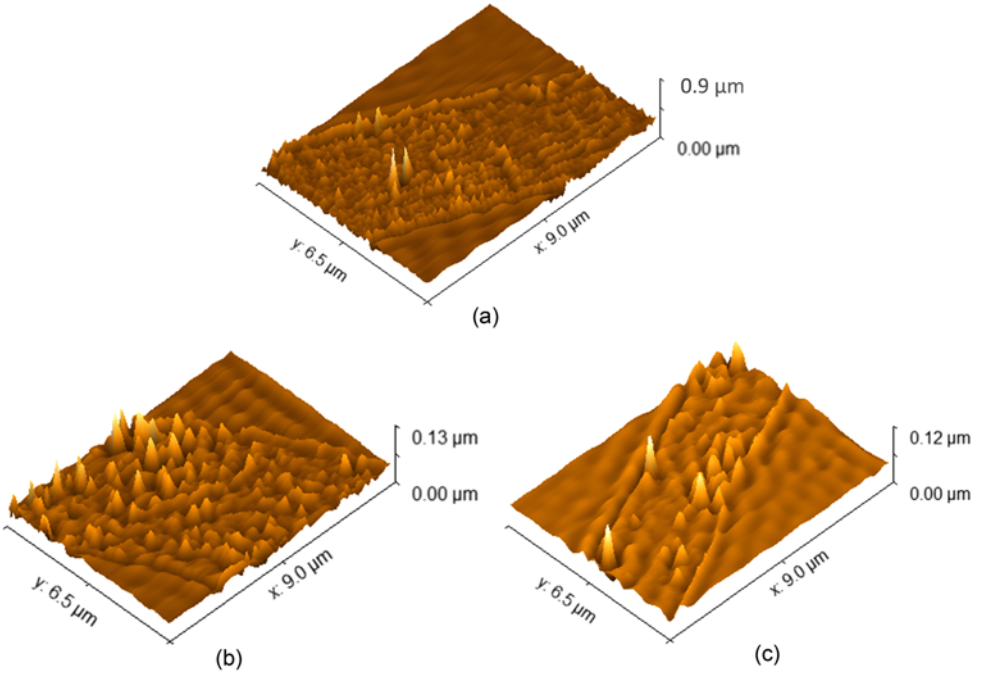

Figure 10. High frequency component atomic force microscopy 3D image of (a) UFPETGO, (b) FAPETGO, and (c) FNPETGO.

of the fibers, which manifest the importance of active functional groups on the substrate surface because the only difference between the substrates was the presence of active functional groups that seems to be important for uniformity and coating uptake.

Conclusion

The role of textiles in electronics is on surge which is further intensified with the invent of graphene based 2D material owing to its exquisite properties. The practical route to fabricate e-textile is by covering the fibre surface with the highly conductive materials in which the interfacial interaction of fibers with coating play a vital role. This investigation highlights the role of functional groups on the fibres surface in increasing the uptake and preventing agglomeration of particles resulting in homogenous coating on the fabrics. The fabrics functionalized with sodium hydroxide showed the highest uptake due to the increase in the wettability and presence of carboxy and hydroxy moeties that form strong covalent bonding of GO with the substrate. Although there is a strong electrostatic attraction between the amine-functionalized positively charged substrate and negatively charged GO, the bonding is strictly physical. The microscopic images and height profiles along with skew and kurtosis values demonstrates that the coating coverage and homogeneity which was found to be the best for samples functionalized with sodium hydroxide, whereas agglomeration was present in the case of untreated samples due to π-π and van der Waals forces acting on unfixed particles resulting in formation of clusters. Further, the improvement in thermal conductivity values manifests the significance of bonding, homogeneity and % uptake of the coating in formation of a conductive network that is paramount for application in e-textiles.

Acknowledgments

The authors would like to express their gratitude to Universiti Sains Malaysia for providing us with a University Research Grant (No:8014044).

References

1. J. Molina, *RSC Adv.*, **6**, 68261 (2016).
2. J. Khan, P. Metrani, and S. Maiti, *J. Emerg. Technol. Innov. Res*., **6**, 836 (2019).
3. F. Shao, N. Hu, Y. Su, L. Yao, B. Li, C. Zou, G. Li, C. Zhang, H. Li, Z. Yang, and Y. Zhang, *Chem. Eng. J*., **392**, 123692 (2020).
4. M. Stoppa and A. Chiolerio, *Sensors (Switzerland)*, **14**, 11957 (2014).
5. G. Chen, Y. Li, M. Bick, and J. Chen, *Chem. Rev.*, **8**, 3668 (2020).
6. M. S. Ersoy, U. Dönmez, K. Yildiz, T. Salan, M. Yazici, İ. Tiyek, and M. H. Alma, *5th Int. Istanbul Text. Congr.*, **5**, 82 (2015).
7. A. I. S. Neves, D. P. Rodrigues, A. De Sanctis, E. T. Alonso, M. S. Pereira, V. S. Amaral, L. V. Melo, S. Russo, I. De Schrijver, H. Alves, and M. F. Craciun, *Sci. Rep*., **7**, 4250 (2017).
8. S. J. Woltornist, F. A. Alamer, A. McDannald, M. Jain, G. A. Sotzing, and D. H. Adamson, *Carbon N. Y.*, **81**, 38 (2015).
9. M. Z. Seyedin, J. M. Razal, P. C. Innis, and G. G. Wallace, *Adv. Funct. Mater*., **24**, 2957 (2014).
10. S. Seyedin, J. M. Razal, P. C. Innis, and G. G. Wallace, *Smart Mater. Struct*., **25**, 035015 (2016).
11. S. Lee, S. Shin, S. Lee, J. Seo, J. Lee, S. Son, H. J. Cho, H. Algadi, S. Al-Sayari, D. E. Kim, and T. Lee, *Adv. Funct. Mater.*, **25**, 3114 (2015).
12. B. Zhang, F. Kang, J. M. Tarascon, and J. K. Kim, *Prog. Mater. Sci*., **76**, 319 (2016).
13. K. Mukai, K. Asaka, X. Wu, T. Morimoto, T. Okazaki, T. Saito, and M. Yumura, *Appl. Phys. Express*, **9**, 055101 (2016).
14. C. Faugeras, B. Faugeras, M. Orlita, M. Potemski, R. R. Nair, and A. K. Geim, *ACS Nano*, **4**, 1889 (2010).
15. A. K. Geim and K. S. Novoselov, *Nat. Mater*., **6**, 183 (2007).
16. X. Hu, Y. Yu, W. Hou, J. Zhou, and L. Song, *Appl. Surf. Sci.*, **273**, 118 (2013).
17. S. F. Kamarudin, M. Mustapha, and J. K. Kim, *Polym. Rev*., **61**, 116 (2020).
18. Y. Z. N. Htwe, I. N. Hidayah, and M. Mariatti, *J. Mater. Sci. Mater. Electron*., **31**, 15361 (2020).
19. S. Pei and H. M. Cheng, *Carbon*, **50**, 3210 (2012).
20. R. Singh, R. D. Kale, T. Potdar, P. Kane, and S. More, *Curr. Graphene Sci.*, **2**, 45 (2018).
21. V. Agarwal and P. B. Zetterlund, *Chem. Eng. J*., **405**, 127018 (2021).
22. J. Khan, S. A. Momin, and M. Mariatti, *Carbon*, **168**, 65 (2020).
23. K. S. Chavali, D. A. Pethsangave, K. C. Patankar, R. V. Khose, P. H. Wadekar, S. Maiti, R. V. Adivarekar, and S. Some, *J. Mater. Sci*., **55**, 14197 (2020).
24. I. A. Sahito, K. C. Sun, A. A. Arbab, M. B. Qadir, and S. H. Jeong, *Electrochim. Acta*, **173**, 164 (2015).
25. W. S. Hummers and R. E. Offeman, *J. Am. Chem. Soc*., **80**, 1339 (1958).
26. D. C. Marcano, D. V. Kosynkin, J. M. Berlin, A. Sinitskii, Z. Sun, A. Slesarev, L. B. Alemany, W. Lu, and J. M. Tour, *ACS Nano*, **4**, 4806 (2010).
27. W. Chen, L. Yan, and P. R. Bangal, *Carbon*, **48**, 1146 (2010).
28. C. Nethravathi and M. Rajamathi, *Carbon*, **46**, 1994 (2008).
29. S. S. Bhattacharya and S. B. Chaudhari, *Int. J. Pure Appl. Sci. Technol*., **21**, 43 (2014).

30. E. Rusu, M. Drobota, and V. Barboiu, *J. Optoelectron. Adv. Mater.*, **10**, 377 (2008).
31. E. Mohammed Khalaf, *Int. J. Mater. Sci. Appl.*, **5**, 297 (2016).
32. Z. Tang, H. Kang, Z. Shen, B. Guo, L. Zhang, and D. Jia, *Macromolecules*, **45**, 3444 (2012).
33. K. Liu, L. Chen, Y. Chen, J. Wu, W. Zhang, F. Chen, and Q. Fu, *J. Mater. Chem.*, **21**, 8612 (2011).
34. D. Kongahge, J. Foroughi, S. Gambhir, G. M. Spinks, and G. G. Wallace, *RSC Adv.*, **6**, 73203 (2016).
35. H. Awais, Y. Nawab, A. Anjang, H. M. Akil, and M. S. Z. Abidin, *Fiber. Polym.*, **21**, 2076 (2020).
36. M. Tian, X. Hu, L. Qu, S. Zhu, Y. Sun, and G. Han, *Carbon*, **96**, 1166 (2016).
37. J. Molina, J. Fernández, M. Fernandes, A. P. Souto, M. F. Esteves, J. Bonastre, and F. Cases, *Synth. Met.*, **202**, 110 (2015).
38. D. Bonn, J. Eggers, J. Indekeu, and J. Meunier, *Rev. Mod. Phys.*, **81**, 739 (2009).
39. M. Clausi, S. Grasselli, A. Malchiodi, and I. S. Bayer, *Appl. Surf. Sci.*, **529**, 147070 (2020).
40. C. Zhao, K. Shu, C. Wang, S. Gambhir, and G. G. Wallace, *Electrochim. Acta*, **172**, 12 (2015).
41. J. A. Moleon, A. Ontiveros-Ortega, E. Gimenez-Martin, and I. Plaza, *Dye Pigment.*, **122**, 310 (2015).
42. X. Tang, M. Tian, L. Qu, S. Zhu, X. Guo, G. Han, K. Sun, X. Hu, Y. Wang, and X. Xu, *Synth. Met.*, **202**, 82 (2015).
43. X. Liu, Z. Qin, Z. Dou, N. Liu, L. Chen, and M. Zhu, *RSC Adv.*, **4**, 23869 (2014).